

RESEARCH ARTICLE OPEN ACCESS

Ultrastructural Insights Into a *Candidatus Parilichlamydia* sp. Infection of Gill Goblet Cells in Greater Amberjack

Maria Chiara Cascarano^{1,2} | Papadogiorgaki Sevasti¹ | Pantelis Katharios² ¹University of Crete, Heraklion, Crete, Greece | ²Institute of Marine Biology, Biotechnology and Aquaculture, Hellenic Centre for Marine Research, Heraklion, Crete, Greece**Correspondence:** Pantelis Katharios (katharios@hcmr.gr)**Received:** 26 February 2025 | **Revised:** 18 April 2025 | **Accepted:** 7 May 2025**Funding:** This study was supported by Hellenic Foundation for Research and Innovation (HFRI) under the HFRI PhD Fellowship grant (Fellowship Number: 253).**Keywords:** *Candidatus Parilichlamydia* | chronic infection | Epitheliocystis | mucous cells | phagoptosis | reservoirs

ABSTRACT

Despite recent genomic studies and increased molecular data, epitheliocystis remains an enigmatic fish disease with no experimental *in vitro* or *in vivo* models to aid the advancement of research. In this study, we revert to a classical microscopical approach and screen with the electron microscope the epitheliocystis lesions caused by a *Ca. Parilichlamydia* sp., infecting mucus cells in Greater amberjack. We report distinct morphological features of this bacterial family, characterised by Intermediate Bodies that closely resemble those of previously described *Candidatus similichlamydia*, and Elementary Bodies that exhibit morphological similarities to *Chlamydia trachomatis*. We describe the characteristics of a novel Chlamydial Inclusion Membrane (IM) type, with abundant interdigitations, possibly shaped by fusion of the IM with cytoplasmic vesicles, and moreover discuss the presence of multivesicular bodies in the infected cell. Our observation of immune cells in the infected areas indicates an interaction of macrophages with infected cells, a role for granular cells as pathogens reservoirs and an active phagoptosis process in the nearby areas, overall shedding light on cellular immune processes characterising these infections in fish hosts.

1 | Introduction

Chlamydial pathogens are highly specialised obligate intracellular Gram-negative bacteria, widely distributed in diverse environments and affecting more than 400 eukaryotic hosts including higher vertebrates, invertebrates and protists (Moulder 2019). These bacteria, which can often reinfect or persist in the organism following first infection (Hogan et al. 2004), target cells of genital, intestinal and ocular mucosal barriers (Premachandra and Jayaweera 2022; Yang et al. 2021), causing characteristic chronic and latent/subclinical infections (Bavoil 2014).

In fish hosts, Chlamydiae have been implicated as causative agents of epitheliocystis disease, a gill and skin infection in which intracellular bacteria cause the distinctive formation of

intracellular inclusions (reviewed in (Blandford et al. 2018)). Six of the nine currently recognised families of the Chlamydial order, *Ca. Piscichlamydiaceae*, *Ca. Clavichamydiaceae*, *Ca. Parilichamydiaceae*, *Parachlamydiaceae*, *Simkaniaceae* and *Rhabdochlamydiaceae*, have been so far associated with the condition (Blandford et al. 2018; Pawlikowska-Warych and Deptuła 2016; Stride et al. 2014), with different bacterial species found in different hosts, overall suggesting a fish host-specificity for these pathogens (Stride et al. 2014). Between these families, the *Candidatus* family *Parilichlamydiaceae*, currently including two proposed genera *Ca. Similichlamydia* and *Ca. Parilichlamydia*, and observed in at least eight fish hosts, has received increasing attention due to its evolutionary significance revealed by its deeply branching position in the Chlamydial taxonomic trees (Stride et al. 2013c;

This is an open access article under the terms of the [Creative Commons Attribution-NonCommercial-NoDerivs](https://creativecommons.org/licenses/by-nc-nd/4.0/) License, which permits use and distribution in any medium, provided the original work is properly cited, the use is non-commercial and no modifications or adaptations are made.

© 2025 The Author(s). *Journal of Fish Diseases* published by John Wiley & Sons Ltd.

Taylor-Brown et al. 2017b). Despite the considerable interest in this chlamydial family and the increasing number of bacteria associated with it, our understanding of these pathogens and their biology remains limited. A few recent studies employing Next-Generation Sequencing (NGS) techniques have shown that those agents have highly reduced genomes characterised by minimal metabolic capacity and enriched in transporters likely used to scavenge nutrients from the host (Pillonel et al. 2018; Taylor-Brown et al. 2018; Taylor-Brown et al. 2017a).

Given the current absence of *in vitro* validation for genomic findings, microscopic observation of the lesions continues to be a crucial tool, albeit limited, to complement the emerging NGS data. One such observation is that lesions associated with Parilichlamydiaceae are observed in different areas of the gill including the filaments and the lamellae, where they seem to cause minimal to no epithelial proliferation in the different fish hosts (Guevara Soto et al. 2016; Seth-Smith et al. 2017; Steigen et al. 2015, 2013; Stride et al. 2013a, 2013b, 2013c; Taylor-Brown et al. 2017a). Moreover, different mechanisms of division of the *Ca. Parilichlamydiaceae* species have been proposed based on both ultrastructural and genomic observations (Pillonel et al. 2018; Seth-Smith et al. 2017), with bacteria dividing by a budding mechanism (Seth-Smith et al. 2017).

Epitheliocystis in Greater Amberjack in Greece has been attributed to two coinfecting bacterial agents, a novel Betaproteobacteria and a *Ca. Parilichlamydia* sp. with 98.64% similarity with *Ca. Parilichlamydia carangidicola* (Cascarano et al. 2022). In this host, two distinct disease manifestations were observed. The acute form involved an infection of interlamellar mitochondria-rich cells (also known as chloride cells), characterised by pronounced focal epithelial proliferation and associated fish mortalities. In contrast, the chronic form presented as a non-proliferative intracellular infection affecting mucous cells along the trailing (afferent) edge of the filament (Cascarano et al. 2022). It should be noted that the term trailing/afferent edge refers to the same area of the filament, the edge which trails the water flow, and it is adjacent to the afferent artery (Wilson and Laurent 2002).

Epitheliocystis infection of mucous cells has been previously described in carp, *Cyprinus carpio*, by Molnar and Boros (1981) and by Paperna and Alves Dematos (1984). These authors provided the first analysis of the ultrastructure of infected mucous cells and investigated the morphology of the infective agents, but were unable to include molecular data, which was not yet accessible at the time. On the other hand, the 16S rRNA is available for the closest relative, the bacteria *Ca. Parilichlamydia carangidicola*, which was described in *Seriola lalandi* in Australia in epithelial cells (Stride et al. 2013a).

While the acute infection of interlamellar chloride cells is currently being attributed to a Beta-proteobacterium (Cascarano M.C. and Katharios P., unpublished data), the chronic infection of mucous cells along the trailing/afferent edge of Greater Amberjack is subject to ultrastructural investigation in the present study. Our aim is to clarify the nature of the infective agent, investigate its intracellular association with the cell

organelles, and explore the local cellular immune response to infection.

2 | Materials and Methods

2.1 | Fish Sampling, Molecular Analysis and Histology

Greater amberjack were sacrificed during an experiment where the onset and progression of epitheliocystis were monitored for over 1 year in cage-reared fish in Souda Bay, Crete, Greece. For extended methods, one can refer to (Cascarano et al. 2022). Briefly, 85 fish from the same fish cohort were sampled in eight different months, following their transfer from a pathogen-free inland hatchery to the sea cages. Gill samples were preserved in 96% ethanol, RNAlater, 10% phosphate buffer formalin and 4F:1G (McDowell and Trump fixative, 4% formaldehyde +1% glutaraldehyde in phosphate buffer), depending on the analysis to perform, which included molecular analysis and histology.

In the aforementioned experiment, fish gills were tested with PCR to detect the presence of bacterial pathogens associated with epitheliocystis using primer sets for known gamma-proteobacteria, beta-proteobacteria and chlamydial agents (Cascarano et al. 2022). Histological analysis was moreover executed in all 85 samples, following gill dehydration and inclusion in glycol methacrylate resin (Technovit 7100; Heraeus Kulzer, Wehrheim, Germany). Sections were obtained by cutting 4 µm gill slices with a microtome (RM 2245; Leica Biosystems, Nussloch, Germany) and stained with methylene blue/azure II/basic fuchsin (polychrome stain) or periodic acid–Schiff (PAS) (Periodic Acid–Schiff (PAS) Stain Kit; Tcs Biosciences, Buckingham, UK). Each sample was screened for the presence of epitheliocystis lesions, marking cyst location along the filament and changes (if any) in the surrounding epithelium (Cascarano et al. 2022).

2.2 | Electron Microscopy

All gill samples in which the distinctive infection of mucous cells along the trailing edge of the filament was observed were retained to select an appropriate sample to process for electron microscopy. To increase the possibility of sectioning infected cells along the thin trailing/afferent edge of the filaments, only samples with abundant cysts were considered. Moreover, gills showing evident coinfection with other bacteria or monogenean parasites were excluded. The chosen sample belonged to a 366 g fish which was sacrificed in December 2018, 4 months after transfer to the sea cages. The gills of this fish were positive for both *Ca. Parilichlamydia* sp. and *Ca. Ichthyocystis* epitheliocystis agents (PCR positive signals) and displayed numerous infected mucous cells, which were observed in almost all filaments (trailing edge and filament tip) of multiple gill arches.

Gills preserved in 4F:1G were rinsed with Sodium Cacodylate Buffer (SCB) (0.1 M, pH 7.2) for 15 min for three times. Following rinsing, gills were fixed with 1% osmium tetroxide for 2 h at RT and rinsed with 0.1 M SCB buffer for 15 min for three times. The fixed sample was dehydrated by ascending grade ethanol

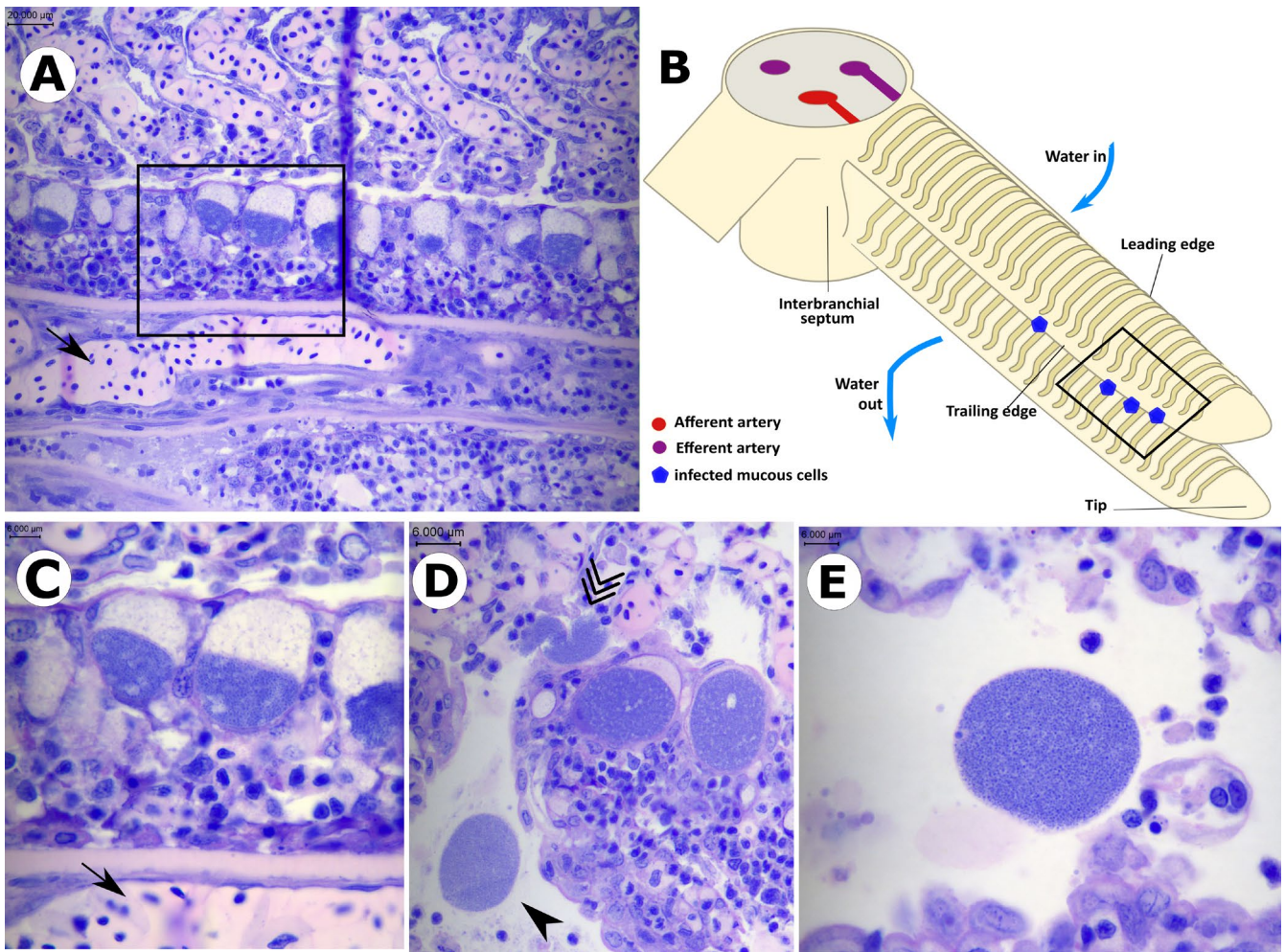


FIGURE 1 | Histology of infected gill filaments, polychrome stain. (A) infected mucous cells in the trailing edge of the filament, above the afferent artery (arrow). (B) Illustration of a partial gill arch (modified from Cascarano et al. 2022) indicating the position of the infected cells. (C) Higher magnification of the area in box A. (D) Rupture of the inclusion and bacterial release (multiple arrowhead), or the whole inclusion detached from the filament (arrowhead). (E) Higher magnification of a detached whole bacterial inclusion.

solutions (30, 50, 70, 80, 90, 95 and 100% ethanol for 15 min for each concentration) and treated with 100% dry ethanol for 20 min, followed by immersion into propylene oxide twice for 15 min each. Following dehydration, filaments from different arches were divided into different blocks and treated with increasing mixed solutions of resin embedding media (Durcupan ACM, Sigma Aldrich) and propylene oxide (V:V = 1:3; V:V = 1:1; V:V = 3:1, for 1 h in each solution) and finally in 100% resin embedding media overnight. The recipe for the resin embedding media included: 10 mL of Durcupan single component A, M epoxy resin; 10 mL of Durcupan single component B, hardener 964; 0.3 mL of Durcupan single component C, accelerator 960 and 0.3 mL Durcupan single component D, plasticiser. Afterwards, the sample was dried at 60°C for 48 h.

Sections were cut from the embedded gills with cross-sections of the trailing/afferent edge and of the filament tip, using an ultramicrotome LEICA EM UC7. Sections were stained with toluidine blue and observed with a light microscope to progressively discard tissues and reach a region of interest. Once a lesion or an area of interest was located, up to three 70 nm thick sections were taken and placed on a copper 300-mesh grid. Samples on

the grid were stained with lead citrate and uranyl acetate and observed in the transmission electron microscope JEOL JEM-2100 (University of Crete) at 80 KV.

3 | Results

Longitudinal sections of the tip and trailing edge of the filaments showed several infected mucous cells often clustering in infected groups (Figure 1A–C). Infected cells were also observed along the trailing edges of multiple neighbouring filaments and in proximity to the interbranchial septum, in areas rich with lymphocytes (Figure 1D). Such cells were never observed along the leading edge.

Infected mucous cells were hypertrophic and showed a distinct polarisation, with intracellular bacteria always observed in an enclosed compartment at the bottom of the cell above the nucleus, and the apical part of the cell filled with mucin granules (Figure 1A,C). In some areas, the rupture of the cyst with release of the bacteria on the epithelium was observed (Figure 1D), or the presence of detached whole bacterial inclusions (Figure 1D,E).

In comparison with the small (up to 20 μm height and 8 μm width), pear-shaped, uninfected neighbouring mucous cells, infected cells are hypertrophic and rounder in shape (up to 28 μm in diameter). The cell morphology changes to accommodate the intracellular expanding bacterial inclusion, which was observed in TEM to range between 5 and 25 μm in diameter. The bacterial compartment progressively fills the cytoplasmic space to the detriment of the upper space available to contain the mucin granules (Figure 2A,B).

We observed the different chlamydial morphological forms in different sizes of inclusion.

Within the smallest observed inclusions (Figure 3A–C), we mostly observed densely aggregated electron-dense chlamydial reticulate bodies (RBs). Two forms of RBs were observed: 1–2 μm elongated dominant bacterial forms with single nucleoids and bigger amorphous multinucleated bacteria (Figure 3B,C). In these inclusions, the interbacterial space appears minimised and RBs are in close contact with one another, tightly wrapped in the inclusion (Figure 3B).

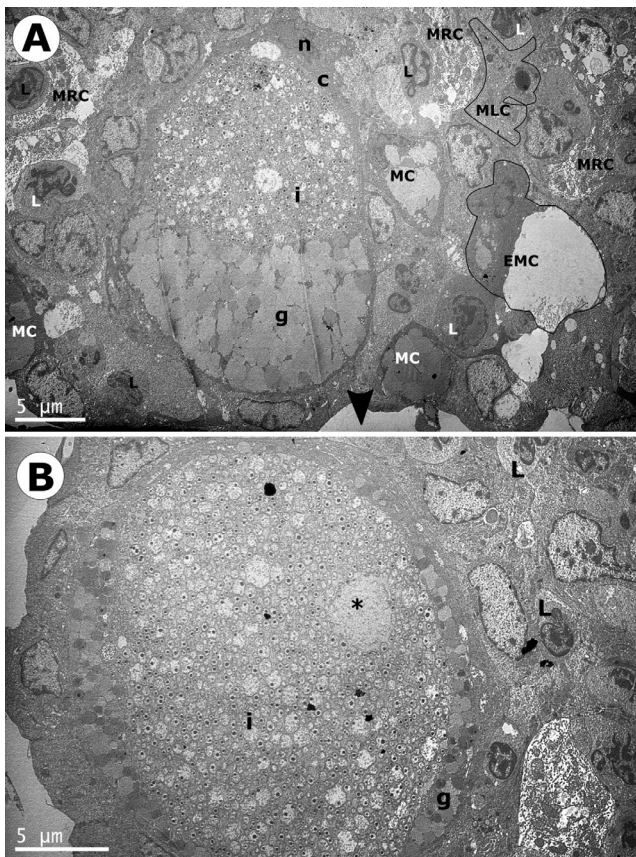


FIGURE 2 | TEM of infected mucous cells with nucleus (n), cytoplasm (c), bacterial inclusion (i) and mucin granules (g). Surrounding cells include lymphocyte-like cells (L), other mucous cells (MC), empty mucous cells (EMC), mitochondria-rich cells (MRC) and migrating macrophage-like cells (MLC). (A) Longitudinal section of infected mucous cell (epithelium surface on the bottom of the picture marked with black arrowhead). (B) Cross-section of an infected cell. In the inclusion (i) note a big aberrant bacterial cell (asterisk).

In the largest inclusions of up to 15 μm (Figure 3D–G), the dominant bacteria morphology is intermediate bodies (IBs), 300–500 nm in diameter, with an electron-dense central nucleoid (100–110 nm) and an electron-dense cytoplasmic area in proximity to the bacterial membrane (Figure 3D). Several amorphous electron-light (toluidine blue unstained) multinuclear 1 μm RBs are moreover observed (Figure 3E). IBs appear to originate by budding of amorphous RBs (Figure 3D) and moreover from binary fission between IBs (Figure 3E). Multiple IBs are observed to be connected by cytoplasmic bridges in a pearl necklace-like structure (Figure 3F). Very few electron-dense elementary bodies (EBs) are observed in the inclusion (Figure 3G). Bacteria are less densely aggregated in the inclusion and the abundant interbacterial space is filled with an electron-dense granular substance (Figure 3D), which is acidophilic when stained in toluidine blue.

In the inclusions above 15 μm (Figure 3H,I) we observed less interbacterial substance with a more granular texture. Amorphous RBs are more regular in shape and appear almost completely spherical (Figure 3H,I). From multinucleate round RBs several IBs originate by budding which also share cytoplasmic bridges (Figure 3H). IBs appear to be smaller, uniform in size (300 nm) and more compact, with few electron-dense cytoplasm around the nucleoid (Figure 3I). Several electron-dense 200 nm EBs originate from IBs in several areas of the inclusion (Figure 3I), wide 4 μm wide aberrant chlamydial bodies can be observed (Figure 2B).

The electron-dense inclusion membrane (IM) surrounds the intracellular space occupied by the replicating bacteria, located between the nucleus (Figure 4A,B) and the above-located mucin granules (Figure 4C,D). In the early stages of replication, when the inclusion is still small and bacterial forms are still prevalently RBs, the inclusion membrane is tightly wrapping the bacteria and its surface is mostly smooth (Figure 3B). With the progression of the infection, bacteria are loosely sparse in the inclusion and often not in contact with the IM (Figure 3B). In this stage, and up to the largest observed inclusions, the inclusion membrane is not smooth but displays numerous characteristic interdigitations of 100–200 nm (Figure 4B). Longer interdigitations with electron-dense granular material are seen in the interface with the nucleus (Figure 4B) and in the upper interface with the mucin granules compartment (Figure 4C).

The electron-dense cytoplasm of the infected cell exhibits numerous electron-light vesicles, approximately 150–200 nm in diameter. These vesicles are particularly prominent beneath the nucleus of the cell (Figure 4A) and in the cytoplasmic periphery of the cell surrounding the granules (Figure 4D). In many areas, such vesicles appear to fuse with the inclusion membrane (Figure 3B).

In other cytoplasmic areas in proximity to the inclusion membrane, we observed multiple membrane stacks/vesicles containing 50–80 nm electron-dense granules (Figure 4E,F). These vesicles are observed to interdigitate and/or fuse with the bacterial inclusion (Figure 4F). The biggest vesicles can reach up to 0.7 μm and resemble multivesicular bodies (Figure 4F).

The inspection of the areas surrounding the infected cells revealed the presence of different cell types, including epithelial cells, lymphocytes, mitochondria-rich cells and migrating macrophages (Figure 2A).

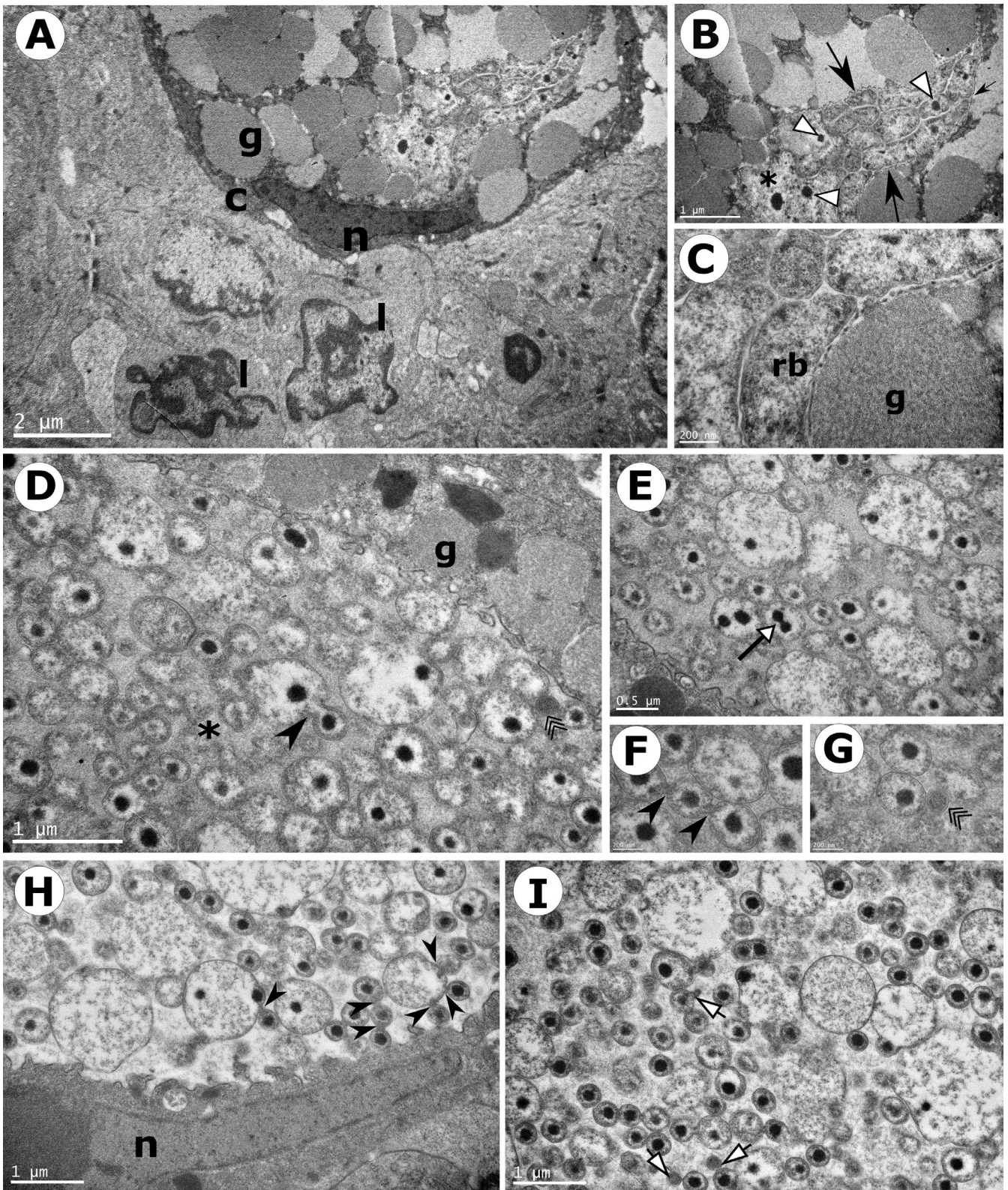


FIGURE 3 | Changes in bacteria morphologies with increasing inclusion size. Inclusion of 5 μm (panel A–C), 14 μm (panels D–G) and 20 μm (H, I). (A) Infected mucous cell with cytoplasm (c), nucleus (n) and mucin granules (g), lymphocyte (l). (B) In between granules (g), an inclusion membrane (black arrowhead) displays tightly packed amorphous bacteria (asterisk) and elongated bacteria with an electron-dense nucleus (white arrowheads). (C) Higher magnification of a reticulate body (RB) above granules (g). (D) Intermediate bodies IB, budding from RB (black arrowhead), intersperse with a dense interbacterial substance (asterisk). Note the presence of few elementary bodies (EB) (multiple arrow). (E) Binary fission between IBs (white arrow). (F) Multiple IBs connected by cytoplasmic bridges (black arrowheads). (G) EB in proximity of IBs (multiple arrow). (H) Several IBs originate from single amorphous polynucleated RB or are connected to each other (black arrowheads). Nucleus (n) of the infected cell. (I) Electron-dense EBs originate from IBs (white arrows).

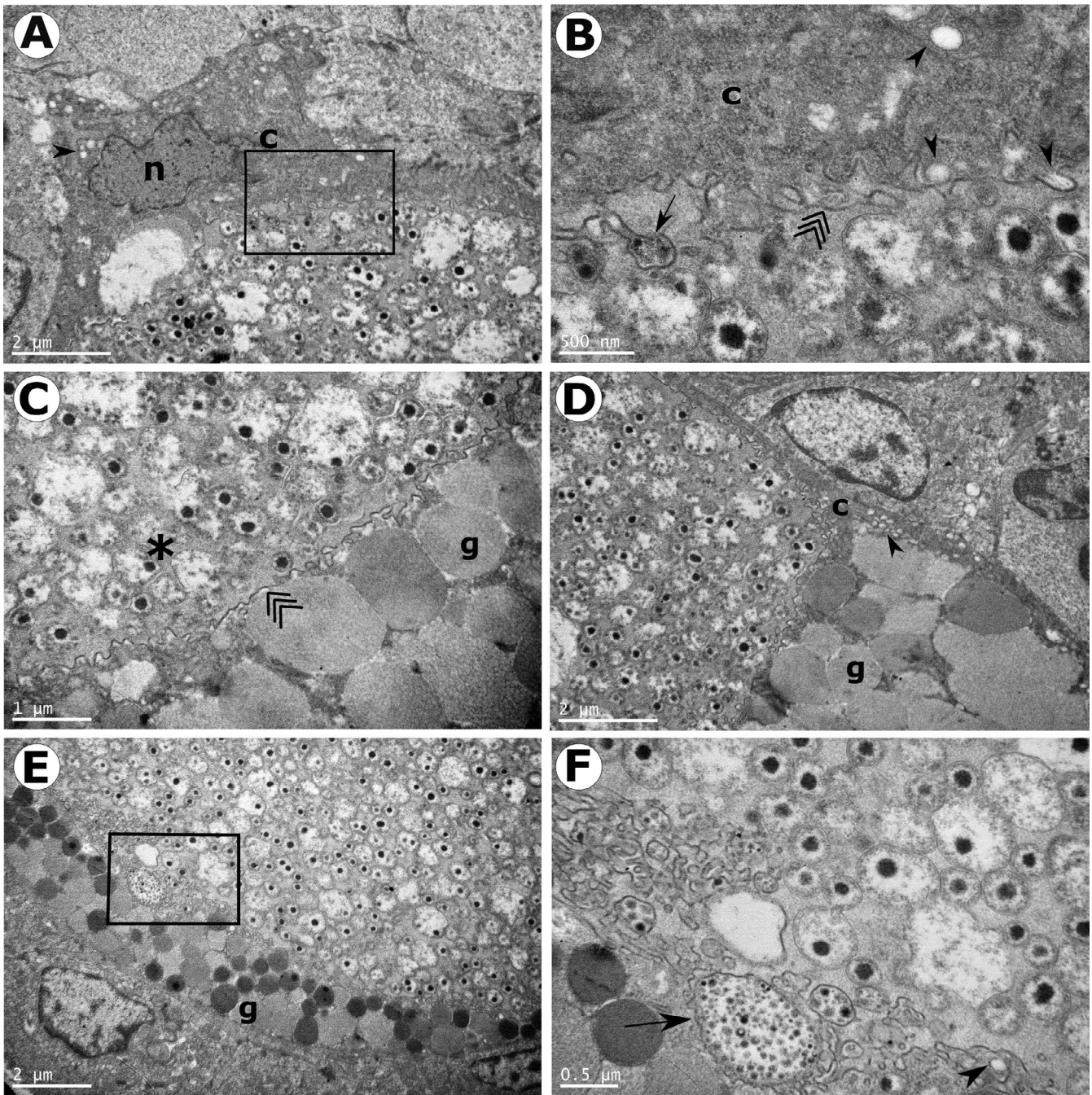


FIGURE 4 | The inclusion membrane. (A) Infected cell with nucleus (n), cytoplasm (c), electron-lucent cytoplasmic vesicles (black arrowhead). (B) Higher magnification of the area in from box A, with cytoplasm (c), and membrane invagination containing electron-dense granular material (black arrow). Note electron-lucent vesicles in the cytoplasm (black arrowheads) fusing with the inclusion membrane (multiple arrow). (C) Interface between inclusion (i) and mucin granules (g) separated by the inclusion membrane (multiple arrow), electron-dense substance in between bacteria (asterisk). (D) Infected cell in the interface between mucin and inclusion; the cytoplasm at the periphery (c) is rich in electron-lucent empty vesicles (black arrowheads). (E) Area with a high number of interdigitations in the inclusion membrane. (F) Higher magnification of the area in the black box E, indicating the presence of a multivesicular body (black arrow) fusing with the inclusion membrane. Electron-lucent vesicles in the cytoplasmic side (black arrowhead).

At least one macrophage with extended pseudopods was observed in proximity to one of the observed infected cells (Figures 2A, 5A). In one specific case, we observed a macrophage cytoplasmic projection adhering to the infected cell (Figure 5B,C). In the adhesion area, the macrophage cytoplasm appears void of organelles and only displays a rough endoplasmic reticulum stack and the presence of small vesicles with electrodense content near the

membrane (Figure 5C). On the other side, the cytoplasm of the infected cell appears more electrodense and has finely granular electrodense particles (Figure 5C).

Below the infected cells, in deeper areas of the filament closer to the afferent artery, we observed some peculiar granulocytes, with toluidine blue-stained basophilic granules (Figure 5D,E).

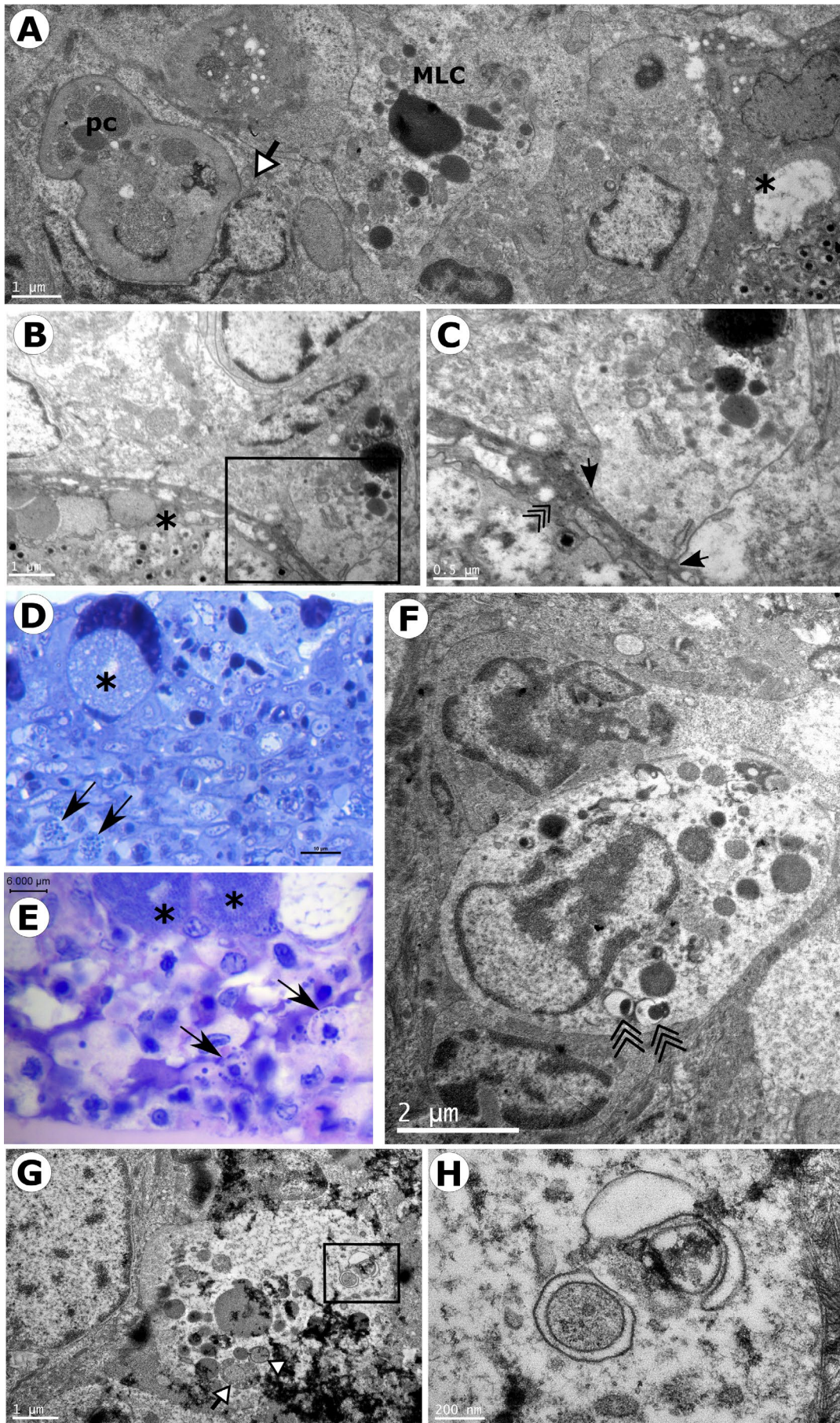


FIGURE 5 | Legend on next page.

FIGURE 5 | Immune cells in proximity of infected mucous cells (asterisk). (A) Macrophage-like cell (MLC) with extending pseudopods and a phagocytic cell (white arrow) displaying in its cytoplasm a phagocytized cell (pc). (B) Interaction between an infected mucous cell and a macrophage. (C) Higher magnification of the area in box B showing the cytoplasmic projection of the macrophage adhering to the infected cell (area between arrows) in proximity of the chlamydial inclusion membrane (multiple arrow). (D) Semithin-section, toluidine blue-stained area between the infected cell and the afferent artery showing granular cells (arrows). (E) Histology polychrome stain of the area between the infected cell and the afferent artery showing granular cells (arrows). (F) TEM of a granular cell with multiple vesicles containing bacterial-like electron-dense peripheral bodies (multiple arrows). (G) Granular cell in proximity of an infected mucous cell, displaying bacteria-like structures inside phagolysosomes (white arrowheads) and in a vesicle (black box). (H) Higher magnification of an area in the black box G. Autophagosome assembles around a cytoplasmic membrane-bound structure, a bacterium is observed in a second vesicle.

These cells always displayed a round-to-oval shape, electron-loose cytoplasm, round-to-oval nucleus with condensed peripheral chromatin, and few granules (Figure 5F). Granules were uniformly electron-dense and regular in most cells, while different sizes and appearances were observed in some cells displaying slight degranulation. In the cytoplasm of these granulocytes, we observed 0.5 to 1 μm electron-lucent membrane-bound vesicles, containing 200–300 nm electrodense bacteria in contact with the vesicle membrane (Figure 5F). In some cases, non-electrodense bacteria could be observed also in lysosomal compartments (Figure 5G), and in phagosomes (Figure 5H).

Other immune cells were detected in the deeper layer of the trailing/afferent edge of the gills, including a number of phagocytic cells digesting whole cells (Figure 6A–D), cells looking like precursors of macrophages (Figure 6E), precursors of granulocytes, and eosinophil-like granulocytes (Figure 6F). As observed in other infected cells (Figure 6B) some of the phagocytized cells resemble mucous or granular cells due to the numerous internal granules (Figure 6C). Cells containing long cytoplasmic projections and bundles of microfilaments were also observed (Figure 6A,B), one of which contained phagocytized cells (Figure 6B).

4 | Discussion

4.1 | The Infecting Agent

What we have previously described as chronic stages of epitheliocystis infection (Casarano et al. 2022) is confirmed here to be a chronic infection of the mucous cells in the mucosal area of the trailing/afferent edge of greater amberjack gill filaments. The intracellular bacteria infecting mucous cells display the typical morphology of a chlamydial agent, and, according to our previous 16S sequencing results, have 98.64% similarity (partial alignment, 79% query cover) with *Ca. Parilichlamydia carangidicola* described from yellowtail kingfish (*Seriola lalandi*) in Australia (Stride et al. 2013a).

The infecting Chlamydial agent displays two forms of RBs, one elongated and the second amorphous and multinucleated (Figure 7A). Elongated RBs were observed only in the smallest inclusions and could therefore represent an initial stage of transition from the primary EB. In the closest observed species of the genus, *Ca. Parilichlamydia carangidicola*, epitheliocystis agent on *Seriola lalandi*, neither EBs nor multinucleated amorphous RBs were observed (Stride et al. 2013a). Even though in the aforementioned study the nature of the infected cell was not

discussed, it is important to underline that chlamydial inclusions were in a central position of the interlamellar area (areas in which also mucous cells are often observed) and that the bacterial infection did not produce a clear proliferative response (Stride et al. 2013a). Closer similarity of RBs was observed with bacteria from *Ca. Similichlamydia* sp. in gilthead seabream in Greece, with similar aberrant bodies and budding of IBs which are observed also connecting by bridges (Seth-Smith et al. 2017). In their study, Seth-Smith and colleagues (Seth-Smith et al. 2017) suggested a shared RBs budding mechanism between Chlamydiae from water vertebrates and observed similarity of *Similichlamydia* RBs with aberrant chlamydial forms produced in other species in the presence of antibiotics or nutrient restrictions (see the study on *C. trachomatis* in (Lambden et al. 2006)). Such observations might be valid also in our case. In the present study, we observed also IBs and few small uniformly electrodense EBs (Figure 7A). Since we did not observe inclusions above 20 μm , we assume that in larger inclusions, a higher ratio of this final infectious stage would be expected. The shape of RBs was not described in *Ca. Parilichlamydia carangidicola* (Stride et al. 2013a) and our findings suggest a clear difference with other members of *Similichlamydia*, *Actinochlamydia* and *Parilichlamydia*, given the fairly uniform round shape and electron-dense granular content appearance of this body, resembling mostly the EBs of *C. trachomatis* (Zigangirova et al. 2013).

We observed a decreasing staining affinity of the chlamydial inclusion with time, with bacteria strongly staining with toluidine blue only at very early stages of infection (small inclusions). In later stages, it might appear that bacteria stain significantly less, while the interbacterial substance inside the inclusion stained blue. We observed that interbacterial material is not observed in small inclusions (densely aggregated RBs only), increases significantly with the appearance of IBs in bigger inclusions and decreases slightly with the appearance of EBs in the biggest inclusion observed.

In carp fry obtained from pond farms in Hungary, Molnar and Boros (Molnar and Boros 1981) described infection of mucous cells with significant similarities to the ones depicted in our study. Interestingly, these authors also observed that the inclusion is stained dark blue in early stages (10–15 μm inclusion, haemalaun and Giemsa stain) and lighter afterwards (70–80 μm) (Molnar and Boros 1981). It was moreover observed that, once the biggest size is reached, the inclusion ‘pushes’ toward the surface of the epithelium, where it can be released with slight compression of the epithelium and, when extruded, it retains its size and shape. Chlamydial bacterial forms described from Hungary resemble closely the IBs observed in our study

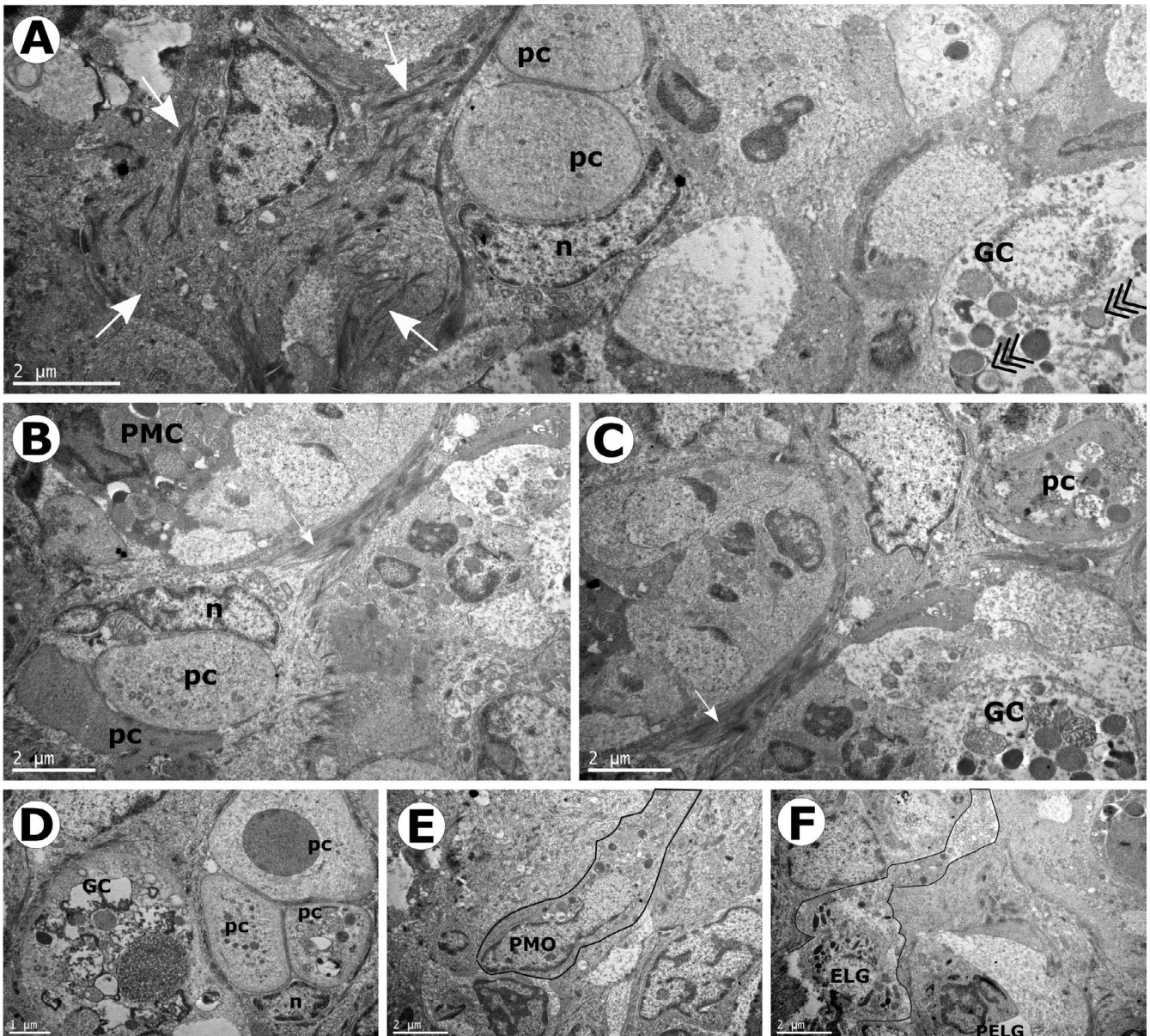


FIGURE 6 | Longitudinal section of the deeper layer of the trailing/afferent edge below infected mucous cell. (A) Granular cell with secondary lysosomes containing either bacteria or secretory granules (multiple arrowhead); Phagocytic cell with nucleus (n) and phagocytized cells (pc); cell with elongated cytoplasmic extensions and numerous cytoplasmic filament bundles (white arrows). (B) Phagocytic cell with nucleus (n) and phagocytized cells (pc). Cytoplasmic projections containing filamentous bundles (white arrow). Nearby a cell resembling the precursor of a mucous cell (PMC). (C) Continuation of the previous picture with filaments in cytoplasmic projection of the phagocytic cell (white arrow), moreover showing another phagocytic cell containing a phagocytized cell (pc) resembling a granular cell or a mucous cell. (D) Degranulating or apoptotic granular cell in proximity of a phagocytic cell with nucleus (n) containing different level of degenerating phagocytized cells (pc). (E) cell resembling a macrophage (PMO). (F) Precursor of eosinophil-like granulocyte with segmented bilobular nucleus (PELG) and an eosinophil-like granulocyte (ELG) with long cytoplasmic projection terminating with several vesicles.

and are even connected in tandems by cytoplasmic bridges. Paperna and Alves Dematos (Paperna and Alves Dematos 1984) observed also similar connections of IBs in the mucous cells of carp farmed in Israel and Portugal. In their study, though, different cell types and many bacterial forms were observed, suggesting also in their case a coinfection of multiple agents. Observation of EBs in carp infected mucocytes, coupled with supporting molecular data, would greatly help the identification of potential phylogenetic relationships between bacteria found in the same cells and different hosts.

4.2 | Intracellular Infection of Mucous Cells

While the study of mucous cells in fish is still in its infancy, we are gathering significant knowledge on their functioning from mammal models. For example, it is now well established that the process of mucus secretion and exocytosis of mucin granules (Burgoyne and Morgan 2003; Verdugo 1990, 1991) is coupled with a mechanism of upper membrane endocytosis to maintain both membrane and secretory potential of the cell in balance and moreover guarantee the continuous secretory

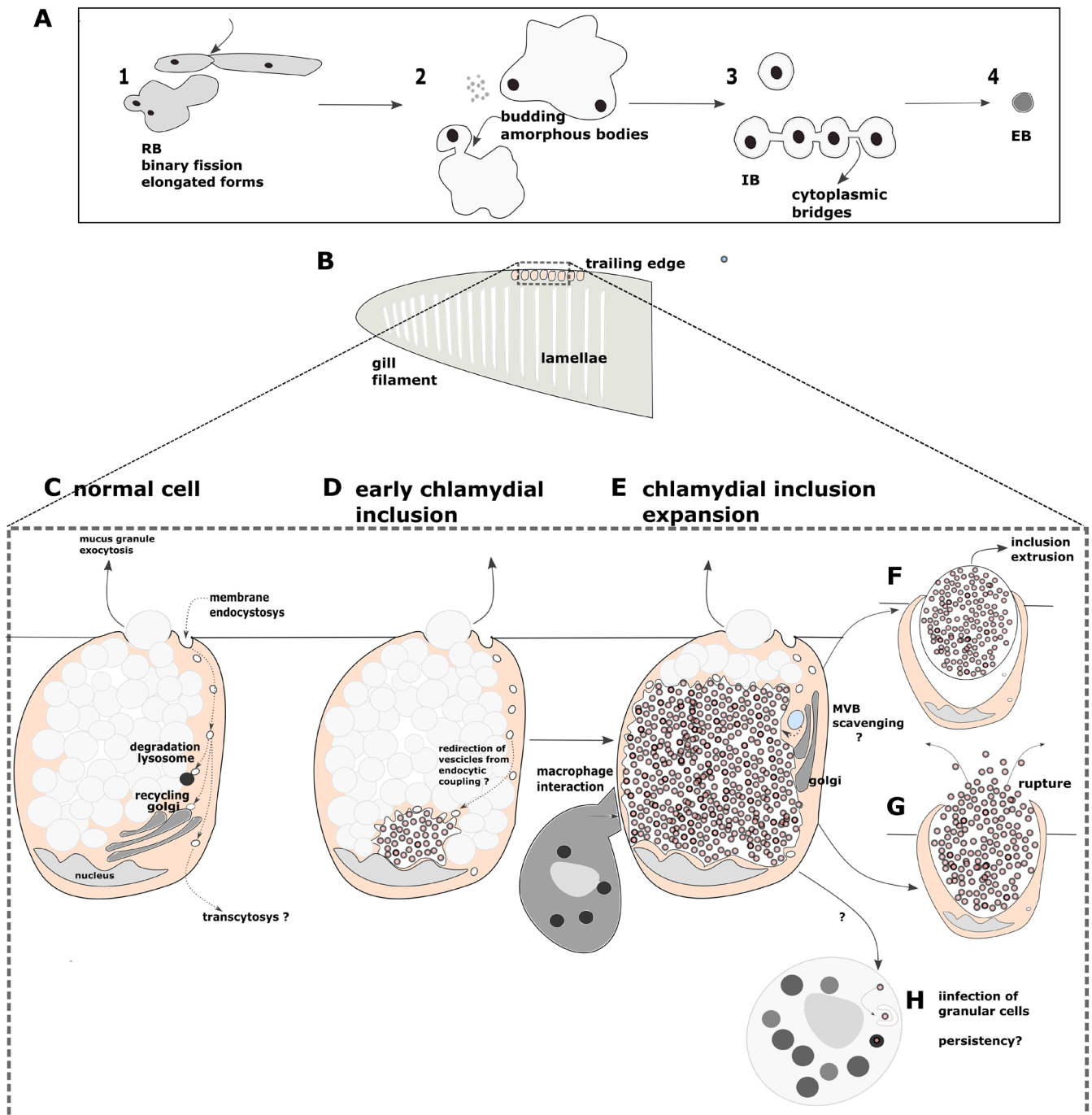


FIGURE 7 | Bacterial morphology and proposed Chlamydial infection cycle inside mucous cells. (A) Variation of bacterial forms within lesion. (1) Reticulate bodies (RB) in elongated forms dividing by binary fission, and amorphous multinucleated forms. Bacteria are closely adhering to each other (no interbacterial space) and have electrodense cytoplasm staining with toluidine blue. (2) Amorphous multinucleated bodies from which intermediate bodies (IB) originate by polar budding. (3) IBs can divide and remain connected by cytoplasmic bridges. (4) Rounded electrodense Elementary bodies (EB). (B) Section of the trailing/afferent edge of the gills where infected mucous cells are to be found. (C) Normal mucous cell showing the exo-endocytic coupling regulating plasma membrane surface balance with endocytic vesicles trafficked to lysosome, Golgi and possibly transcytosis. (D) Early chlamydial inclusion developing above the cell nucleus, possibly redirecting endocytic vesicles to the inclusion. (E) Expansion of the chlamydial inclusion and possible fusion of multivesicular body (MVB) blue vesicle, with inclusion membrane. Note the interaction with the adhering macrophage. (F) Extrusion of the inclusion in the water, as observed in previous studies (Cascarano et al. 2022). (G) Rupture of the cyst releasing bacteria on the epithelium as observed in previous studies (Cascarano et al. 2022). (H) Putative secondary infection of granular cells.

capabilities of the cell (Gundelfinger et al. 2003). Such ‘recycling’ of portions of the cytoplasmic membrane in secreting cells (a process known as exo-endocytosis coupling) has been discussed in mice intestinal goblet cells, where it has been

shown that parts of the secretory granule membrane are re-endocytosed after granule secretion and trafficked to either lysosomes (for degradation), Golgi (for membrane recycling) or even transited to other cells for immune processing of the

external lumen contents (transcytosis) (Gustafsson et al. 2021) (Figure 7C).

In our study, we did observe the presence of small empty vesicles in the upper cytoplasmic membrane of uninfected mucocytes in proximity to the mucus secretion pore (not shown). Size and shape of such vesicles resemble the numerous small vesicles found in proximity to the IM in infected cells, which seem, at different points, to fuse with the inclusion, forming the characteristic invaginations. We moreover observed that the shape of the IM changes over time, with bigger inclusions displaying an increased number of IM interdigitations, and a lower number of surface mucin granules. While a completely different kind of study is necessary to prove the ability of Chlamydiae to scavenge endocytic vesicles from the exo-endocytic coupling in our model, it is well known that intracellular bacteria require host cell membrane to expand their intracellular niche during replication (Case et al. 2016). Our hypothesis is that, if *Ca. Parilichlamydia* could redirect endocytic vesicles, less membrane would be available for mucin granule production and, instead, would be available for the expansion of the inclusion, explaining the simultaneous increase in size of IM and decrease in mucus content of the infected cell (Figure 7D,E). Consequently, the chlamydial agent could be actively interfering with mucin granules formation and mucus secretion during infection, with multiple implications in the disease development.

Aside from the membrane surface, obligate intracellular bacteria need to scavenge nutrients from the host cell. In other Chlamydial studies, it has been shown that bacterial effectors secreted and inserted in the IM, the inclusion membrane proteins (INCs), can promote nutrient acquisition through redirection of cell nutrient-rich exocytic vesicles transiting from the Golgi apparatus, or trafficking of multivesicular bodies (MVB) (Elwell et al. 2016). Multivesicular bodies are specialised heterogeneous late endosomes that include proteins and lipids to be recycled, degraded or expelled from the cell (Denzer et al. 2000; Piper and Luzio 2001). In *C. trachomatis*, MVBs are hijacked by the bacteria and their content is delivered into the bacterial inclusion to promote bacterial intracellular development and, moreover, for the reactivation of persistent bacteria (Beatty 2006, 2008; Gambarte Tudela et al. 2015; Robertson et al. 2009). Importantly, in mucous cells, glycoproteins, which are necessary to form the mucin granules, are also trafficked from the Golgi (Neutra and Leblond 1966). In our work, we observed a chlamydial inclusion containing RBs and IBs to be in contact with vesicles containing electron-dense granules resembling MVBs. While the fusion and nature of such compartments is far from being demonstrated for these non-cultivable bacteria, our observations suggest the possibility of a common mechanism of scavenging late endosomes in *Ca. Parilichlamydia* and *C. trachomatis* (Figure 7E). Moreover, if the intracellular bacteria could indeed redirect vesicles from the Golgi, it could also be scavenging mucin precursors.

In the absence of in vivo infection models, it is not possible to state if the extrusion of the whole bacterial inclusion observed in histology (Casarano et al. 2022), and similarly noted in carp (Molnar and Boros 1981), is just a post-mortem artefact. Aside from the abundant evidence of detached whole cysts in our samples, we do consider cyst extrusion a possibility because such

a mechanism is described as a conserved exit mechanism in other Chlamydial species (Zuck, Sherrid, et al. 2016). Extrusion of whole inclusion has been shown in detail in *C. trachomatis* (Volceanov et al. 2014) and is believed to be a strategy aiming to increase bacterial survival outside the infected cell and assist transmission to other cells, or even other hosts (Hybiske and Stephens 2007). Whole extruded chlamydial inclusions have been moreover proved to be engulfed and disseminated in other areas by macrophages (Zuck, Ellis, et al. 2016).

4.3 | Local Cellular Immune Response to Chlamydial Infection

Macrophages, which are known to populate gills mucosal tissue (Koppang et al. 2015), can be additionally recruited from other areas by proinflammatory signals, as it has been described in *C. trachomatis* (reviewed in (Lausen et al. 2019)). Activated macrophages migrate with chemotaxis to infected areas in response to different stimuli, moving using pseudopods and mobile processes (Mathias et al. 2009; Rougerie et al. 2013). They perform various tasks and can have a direct cytotoxic effect on damaged or virus-infected cells, or facilitate cytotoxic action by activating lymphocytes (Alexander and Evans 1971; Corthay et al. 2005; Haabeth et al. 2011; Porta et al. 2015) through Toll-like receptor and interferon pathways (Müller et al. 2017). Macrophages are also potential host cells susceptible to infection, as it has been shown that other chlamydial species can survive phagocytosis and reside (but not replicate) in these cells, making them possible vehicles for bacterial dissemination (Herweg and Rudel 2016). In our study, a thorough comparison with uninfected gills is missing, which would have helped in discriminating between resident immune cell populations and immune cells migrating in the area during infection. Nevertheless, at least one macrophage was observed in proximity to every chlamydia-infected cell, with one macrophage even showing an area of adhesion to an infected cell (Figure 7E). Even if additional studies are necessary to support this observation, the direct contact between macrophage and infected mucous cell shown here suggests a direct cytotoxic action by transfer of cytotoxic compounds. Importantly, none of the inspected macrophages was observed to contain chlamydial bodies, while we observed non-replicating bacteria inside granular cells.

In proximity to the infected cells and in deeper layers of the filament, we observed several cells that were described as phagocytic cells containing whole cells. Such description was made based on the observation of cells including large phagosomes containing whole degrading cells (resembling mucous cells or granular cells) and, moreover, for similarity to the mononuclear phagocytes engulfing eukaryotic cells described in fish spleen (Dyková et al. 2022). Phagoptosis (or primary phagocytosis) is the killing of a viable cell by phagocytosis which is related to the expression of specific 'eat me signals' following stress, damage or senescence of the cell (Brown and Neher 2012); associated with biological processes as cell turnover, regulation of inflammation and defence against pathogens and cancer cells (Brown and Neher 2012; Brown et al. 2015). While this process has been extensively studied in mammals, it was predicted to be the subject of future studies in teleost (Esteban et al. 2015), where it has been related to apoptotic cell clearance in zebrafish models

(Blume et al. 2020). It is interesting to notice that in our study most phagocytized cells resemble mucous or granular cells. Considering that both these cell types have been shown to be putatively infected by the *Ca. Parilichlamydia* agent, this could lead us to hypothesise that infected cells are recognised and targeted by immune phagocytic cells and that phagoptosis is part of the mechanisms activated during chlamydial infection of cells in fish gills.

A number of granular cells were observed in the deeper layer of the trailing/afferent edge of the gills, below the layer of infected cells, of which a few displayed some degree of degranulation. In our study, we pointed to the presence of one or two different types of bacteria (based on different electron-density) inside lysosomal compartments or in endocytic vesicles in cells neighbouring chlamydial-infected cells. Considering that our screened sample was positive for two different agents, we suggest that one or even both epitheliocystis agents infecting greater amberjack could transit or reside in these cells, with proximity to infected mucous cells mostly supporting this evidence for the chlamydial agent. The presence of non-replicating bacteria in infected immune cells can cause persistency of the agents in the tissues following the first infection (Hogan et al. 2004), and might explain the prolonged observation of Chlamydial signal obtained by PCR screening during our previous monitoring study (Casarano et al. 2022).

Based on this study and our previous observations in histology (Casarano et al. 2022), extrusion of whole inclusions from the epithelium, rupture of the inclusions with bacterial dissemination on the epithelia and persistence in immune cells can all be potential means of transmission and dissemination of this chlamydial pathogen (Figure 7F–H).

Author Contributions

Maria Chiara Casarano: conceptualization, investigation, methodology, validation, visualization, formal analysis, writing – review and editing, writing – original draft. **Papadogiorgaki Sevasti:** investigation, methodology, visualization, writing – review and editing, formal analysis. **Pantelis Katharios:** conceptualization, investigation, methodology, writing – original draft, writing – review and editing, funding acquisition, supervision, formal analysis.

Acknowledgements

The study was partially supported by the Hellenic Foundation for Research and Innovation (HFRI) under the HFRI PhD Fellowship grant (Fellowship Number: 253). The authors would like to dedicate it to the late Professor Lloyd Vaughan for his encouragement and passionate support, which contributed to the development of this research. Additionally, our gratitude extends to Dr Ivona Mladineo for her valuable inputs during the initial revisions of this manuscript and to the anonymous reviewers who helped reshape its structure.

Conflicts of Interest

The authors declare no conflicts of interest.

Data Availability Statement

The data supporting this study are available upon reasonable request from the authors. Requests can be made via email to the corresponding author.

References

- Alexander, P., and R. Evans. 1971. “Endotoxin and Double Stranded RNA Render Macrophages Cytotoxic.” *Nature: New Biology* 232, no. 29: 76–78.
- Bavoil, P. M. 2014. “What’s in a Word: The Use, Misuse, and Abuse of the Word “Persistence” in Chlamydia Biology.” *Frontiers in Cellular and Infection Microbiology* 4: 27.
- Beatty, W. L. 2006. “Trafficking From CD63-Positive Late Endocytic Multivesicular Bodies Is Essential for Intracellular Development of *Chlamydia trachomatis*.” *Journal of Cell Science* 119, no. 2: 350–359. <https://doi.org/10.1242/jcs.02733>.
- Beatty, W. L. 2008. “Late Endocytic Multivesicular Bodies Intersect the Chlamydial Inclusion in the Absence of CD63.” *Infection and Immunity* 76, no. 7: 2872–2881.
- Blandford, M. I., A. Taylor-Brown, T. A. Schlacher, B. Nowak, and A. Polkinghorne. 2018. “Epitheliocystis in Fish: An Emerging Aquaculture Disease With a Global Impact.” *Transboundary and Emerging Diseases* 65: 1436–1446. <https://doi.org/10.1111/tbed.12908>.
- Blume, Z. I., J. M. Lambert, A. G. Lovel, and D. M. Mitchell. 2020. “Microglia in the Developing Retina Couple Phagocytosis With the Progression of Apoptosis via P2RY12 Signaling.” *Developmental Dynamics* 249, no. 6: 723–740.
- Brown, G. C., and J. Neher. 2012. “Eaten Alive! Cell Death by Primary Phagocytosis: ‘Phagoptosis.’” *Trends in Biochemical Sciences* 37, no. 8: 325–332.
- Brown, G. C., A. Vilalta, and M. Fricker. 2015. “Phagoptosis-Cell Death by Phagocytosis-Plays Central Roles in Physiology, Host Defense and Pathology.” *Current Molecular Medicine* 15, no. 9: 842–851.
- Burgoyne, R. D., and A. Morgan. 2003. “Secretory Granule Exocytosis.” *Physiological Reviews* 83, no. 2: 581–632.
- Casarano, M. C., M. Ruetten, L. Vaughan, et al. 2022. “Epitheliocystis in Greater Amberjack: Evidence of a Novel Causative Agent, Pathology, Immune Response and Epidemiological Findings.” *Microorganisms* 10, no. 3: 627. <https://doi.org/10.3390/microorganisms10030627>.
- Case, E. D. R., J. A. Smith, T. A. Ficht, J. E. Samuel, and P. de Figueiredo. 2016. “Space: A Final Frontier for Vacuolar Pathogens.” *Traffic* 17, no. 5: 461–474.
- Corthay, A., D. K. Skovseth, K. U. Lundin, et al. 2005. “Primary Antitumor Immune Response Mediated by CD4+ T Cells.” *Immunity* 22, no. 3: 371–383. <https://doi.org/10.1016/j.immuni.2005.02.003>.
- Denzer, K., M. J. Kleijmeer, H. F. Heijnen, W. Stoorvogel, and H. J. Geuze. 2000. “Exosome: From Internal Vesicle of the Multivesicular Body to Intercellular Signaling Device.” *Journal of Cell Science* 113, no. 19: 3365–3374.
- Dyková, I., J. Žák, R. Blažek, M. Reichard, K. Součková, and O. Slabý. 2022. “Histology of Major Organ Systems of Nothobranchius Fishes: Short-Lived Model Species.” *Journal of Vertebrate Biology* 71, no. 21074: 21071–21074. <https://doi.org/10.25225/jvb.21074>.
- Elwell, C., K. Mirrashidi, and J. Engel. 2016. “Chlamydia Cell Biology and Pathogenesis.” *Nature Reviews Microbiology* 14, no. 6: 385–400.
- Esteban, M. Á., A. Cuesta, E. Chaves-Pozo, and J. Meseguer. 2015. “Phagocytosis in Teleosts. Implications of the New Cells Involved.” *Biology* 4, no. 4: 907–922.
- Gambarte Tudela, J., A. Capmany, M. Romao, et al. 2015. “The Late Endocytic Rab39a GTPase Regulates the Interaction Between Multivesicular Bodies and Chlamydial Inclusions.” *Journal of Cell Science* 128, no. 16: 3068–3081. <https://doi.org/10.1242/jcs.170092>.
- Guevara Soto, M., B. Vidondo, L. Vaughan, et al. 2016. “The Emergence of Epitheliocystis in the Upper Rhone Region: Evidence for Chlamydiae in Wild and Farmed Salmonid Populations.” *Archives of Microbiology* 198: 315–324.

- Gundelfinger, E. D., M. M. Kessels, and B. Qualmann. 2003. "Temporal and Spatial Coordination of Exocytosis and Endocytosis." *Nature Reviews Molecular Cell Biology* 4, no. 2: 127–139.
- Gustafsson, J. K., J. E. Davis, T. Rappai, et al. 2021. "Intestinal Goblet Cells Sample and Deliver Luminal Antigens by Regulated Endocytic Uptake and Transcytosis." *eLife* 10: e67292. <https://doi.org/10.7554/eLife.67292>.
- Haabeth, O. A. W., K. B. Lorvik, C. Hammarström, et al. 2011. "Inflammation Driven by Tumour-Specific Th1 Cells Protects Against B-Cell Cancer." *Nature Communications* 2, no. 1: 1–12.
- Herweg, J., and T. Rudel. 2016. "Interaction of Chlamydiae With Human Macrophages." *FEBS Journal* 283, no. 4: 608–618.
- Hogan, R. J., S. A. Mathews, S. Mukhopadhyay, J. T. Summersgill, and P. Timms. 2004. "Chlamydial Persistence: Beyond the Biphasic Paradigm." *Infection and Immunity* 72, no. 4: 1843–1855.
- Hybiske, K., and R. S. Stephens. 2007. "Mechanisms of Host Cell Exit by the Intracellular Bacterium Chlamydia." *Proceedings of the National Academy of Sciences* 104, no. 27: 11430–11435.
- Koppang, E. O., A. Kvellestad, and U. Fischer. 2015. "Fish Mucosal Immunity: Gill." In *Mucosal Health in Aquaculture*. Academic Press. <https://doi.org/10.1016/B978-0-12-417186-2.00005-4>.
- Lambden, P. R., M. A. Pickett, and I. N. Clarke. 2006. "The Effect of Penicillin on *Chlamydia trachomatis* DNA Replication." *Microbiology* 152, no. 9: 2573–2578.
- Lausen, M., G. Christiansen, T. B. G. Poulsen, and S. Birkelund. 2019. "Immunobiology of Monocytes and Macrophages During *Chlamydia trachomatis* Infection." *Microbes and Infection* 21, no. 2: 73–84.
- Mathias, J. R., M. E. Dodd, K. B. Walters, S. K. Yoo, E. A. Ranheim, and A. Huttenlocher. 2009. "Characterization of Zebrafish Larval Inflammatory Macrophages." *Developmental & Comparative Immunology* 33, no. 11: 1212–1217.
- Molnar, K., and G. Boros. 1981. "A Light and Electron Microscopic Study of the Agent of Carp Mucophilosis." *Journal of Fish Diseases* 4, no. 4: 325–334.
- Moulder, J. W. 2019. "Characteristics of Chlamydiae." In *Microbiology of Chlamydia*, edited by J. W. Moulder, 3–19. CRC Press.
- Müller, E., P. F. Christopoulos, S. Halder, et al. 2017. "Toll-Like Receptor Ligands and Interferon- γ Synergize for Induction of Antitumor M1 Macrophages." *Frontiers in Immunology* 8: 1383. <https://doi.org/10.3389/fimmu.2017.01383>.
- Neutra, M., and C. P. Leblond. 1966. "Synthesis of the Carbohydrate of Mucus in the Golgi Complex as Shown by Electron Microscope Radioautography of Goblet Cells From Rats Injected With Glucose-H₃." *Journal of Cell Biology* 30, no. 1: 119–136.
- Paperna, I., and A. P. Alves Dematos. 1984. "The Developmental Cycle of Epitheliocystis in Carp, *Cyprinus carpio* L." *Journal of Fish Diseases* 7, no. 2: 137–147.
- Pawlikowska-Warych, M., and W. Deptuła. 2016. "Characteristics of Chlamydia-Like Organisms Pathogenic to Fish." *Journal of Applied Genetics* 57: 135–141.
- Pillonel, T., C. Bertelli, and G. Greub. 2018. "Environmental Metagenomic Assemblies Reveal Seven New Highly Divergent Chlamydial Lineages and Hallmarks of a Conserved Intracellular Lifestyle." *Frontiers in Microbiology* 9: 314120.
- Piper, R. C., and J. P. Luzio. 2001. "Late Endosomes: Sorting and Partitioning in Multivesicular Bodies." *Traffic* 2, no. 9: 612–621.
- Porta, C., E. Riboldi, A. Ippolito, and A. Sica. 2015. "Molecular and Epigenetic Basis of Macrophage Polarized Activation." In *Seminars in Immunology*, vol. 27, 237–248. Elsevier.
- Premachandra, N. M., and J. A. A. S. Jayaweera. 2022. "*Chlamydia pneumoniae* Infections and Development of Lung Cancer: Systematic Review." *Infectious Agents and Cancer* 17, no. 1: 11.
- Robertson, D. K., L. Gu, R. K. Rowe, and W. L. Beatty. 2009. "Inclusion Biogenesis and Reactivation of Persistent *Chlamydia trachomatis* Requires Host Cell Sphingolipid Biosynthesis." *PLoS Pathogens* 5, no. 11: e1000664.
- Rougerie, P., V. Miskolci, and D. Cox. 2013. "Generation of Membrane Structures During Phagocytosis and Chemotaxis of Macrophages: Role and Regulation of the Actin Cytoskeleton." *Immunological Reviews* 256, no. 1: 222–239.
- Seth-Smith, H. M. B., P. Katharios, N. Dourala, et al. 2017. "*Ca*. Similichlamydia in Epitheliocystis Co-Infection of Gilthead Seabream Gills: Unique Morphological Features of a Deep Branching Chlamydial Family." *Frontiers in Microbiology* 8, no. MAR: 1–9. <https://doi.org/10.3389/fmicb.2017.00508>.
- Steigen, A., E. Karlsbakk, H. Plarre, et al. 2015. "A New Intracellular Bacterium, *Candidatus* Similichlamydia Labri sp. nov. (Chlamydiaceae) Producing Epitheliocysts in Ballan Wrasse, *Labrus bergylta* (Pisces, Labridae)." *Archives of Microbiology* 197, no. 2: 311–318.
- Steigen, A., A. Nylund, E. Karlsbakk, et al. 2013. "Cand. Actinochlamydia Clariae' gen. nov., sp. nov., a Unique Intracellular Bacterium Causing Epitheliocystis in Catfish (*Clarias gariepinus*) in Uganda." *PLoS One* 8, no. 6: e66840. <https://doi.org/10.1371/journal.pone.0066840>.
- Stride, M. C., A. Polkinghorne, T. L. Miller, J. M. Groff, S. E. LaPatra, and B. F. Nowak. 2013a. "Molecular Characterization of "*Candidatus* Parilichlamydia Carangidicola," a Novel Chlamydia-Like Epitheliocystis Agent in Yellowtail Kingfish, *Seriola lalandi* (Valenciennes), and the Proposal of a New Family, "*Candidatus* Parilichlamydiaceae" Fam. nov." *Applied and Environmental Microbiology* 79, no. 5: 1590–1597. <https://doi.org/10.1128/AEM.02899-12>.
- Stride, M. C., A. Polkinghorne, T. L. Miller, and B. F. Nowak. 2013b. "Molecular Characterization of "*Candidatus* Similichlamydia Latridicola" Gen. nov., sp. nov. (Chlamydiales: "*Candidatus* Parilichlamydiaceae"), a Novel Chlamydia-Like Epitheliocystis Agent in the Striped Trumpeter, *Latris lineata* (Forster)." *Applied and Environmental Microbiology* 79, no. 16: 4914–4920.
- Stride, M. C., A. Polkinghorne, and B. F. Nowak. 2014. "Chlamydial Infections of Fish: Diverse Pathogens and Emerging Causes of Disease in Aquaculture Species." *Veterinary Microbiology* 171, no. 1–2: 258–266. <https://doi.org/10.1016/j.vetmic.2014.03.022>.
- Stride, M. C., A. Polkinghorne, M. D. Powell, and B. F. Nowak. 2013c. "*Candidatus* Similichlamydia Laticola", a Novel Chlamydia-Like Agent of Epitheliocystis in Seven Consecutive Cohorts of Farmed Australian Barramundi, *Lates calcarifer* (Bloch)." *PLoS One* 8, no. 12: e82889. <https://doi.org/10.1371/journal.pone.0082889>.
- Taylor-Brown, A., T. Pillonel, A. Bridle, et al. 2017a. "Culture-Independent Genomics of a Novel Chlamydial Pathogen of Fish Provides New Insight Into Host-Specific Adaptations Utilized by These Intracellular Bacteria." *Environmental Microbiology* 19, no. 5: 1899–1913. <https://doi.org/10.1111/1462-2920.13694>.
- Taylor-Brown, A., T. Pillonel, G. Greub, L. Vaughan, B. Nowak, and A. Polkinghorne. 2018. "Metagenomic Analysis of Fish-Associated *Ca*. Parilichlamydiaceae Reveals Striking Metabolic Similarities to the Terrestrial Chlamydiaceae." *Genome Biology and Evolution* 10, no. 10: 2587–2595.
- Taylor-Brown, A., L. Spang, N. Borel, and A. Polkinghorne. 2017b. "Culture-Independent Metagenomics Supports Discovery of Uncultivable Bacteria Within the Genus Chlamydia." *Scientific Reports* 7, no. 1: 10661.
- Verdugo, P. 1990. "Goblet Cells Secretion and Mucogenesis." *Annual Review of Physiology* 52, no. 1: 157–176.

- Verdugo, P. 1991. "Mucin Exocytosis1-3." *American Review of Respiratory Disease* 144: S33-S37.
- Volceanov, L., K. Herbst, M. Biniossek, et al. 2014. "Septins Arrange F-Actin-Containing Fibers on the *Chlamydia trachomatis* Inclusion and Are Required for Normal Release of the Inclusion by Extrusion." *MBio* 5, no. 5: 10-1128.
- Wilson, J. M., and P. Laurent. 2002. "Fish Gill Morphology: Inside Out." *Journal of Experimental Zoology* 293, no. 3: 192-213.
- Yang, X., A. Siddique, A. A. Khan, et al. 2021. "*Chlamydia trachomatis* Infection: Their Potential Implication in the Etiology of Cervical Cancer." *Journal of Cancer* 12, no. 16: 4891-4900. <https://doi.org/10.7150/jca.58582>.
- Zigangirova, N. A., Y. P. Rumyantseva, E. Y. Morgunova, et al. 2013. "Detection of *C. trachomatis* in the Serum of the Patients With Urogenital Chlamydiosis." *BioMed Research International* 2013: 489489.
- Zuck, M., T. Ellis, A. Venida, and K. Hybiske. 2016. "Extrusions Promote Engulfment and Chlamydia Survival Within Macrophages." *BioRxiv* 19: e12683.
- Zuck, M., A. Sherrid, R. Suchland, T. Ellis, and K. Hybiske. 2016. "Conservation of Extrusion as an Exit Mechanism for Chlamydia." *Pathogens and Disease* 74, no. 7: ftw093. <https://doi.org/10.1093/femspd/ftw093>.